G. P. Gilfoyle

Few-Body Physics with CLAS

Abstract The study of few-body, nuclear systems with electromagnetic probes is an essential piece of the scientific program at Jefferson Lab. Reactions using real photons and electrons (up to energies of 6 GeV) are measured using the CEBAF large acceptance spectrometer (CLAS) detector in Hall B, a nearly 4π magnetic spectrometer. We focus here on three areas. (1) Short-range correlations (SRCs) probe the high-momentum components of the nuclear wave function. Recent CLAS experiments map out their isospin character and reveal the importance of the tensor part of the nuclear force. (2) Three-body forces are an essential feature of nuclei. We will show results using real photons and ^{3}He and ^{4}He targets that remain largely unexplained. (3) Evidence for the transition to a quark-gluon description of nuclei has been observed with photon beams in CLAS on deuterium and 3-He targets. Alternative explanations reveal the geography of the transition is complex.

1 Introduction

The atomic nucleus provides us with a laboratory to study few-body physics among the nucleons and their constituents, the quarks and gluons. The CEBAF large acceptance spectrometer (CLAS) detector at the Thomas Jefferson National Accelerator Facility (JLab) has a strong program in this area to support the JLab mission. In particular, we seek to understand what QCD reveals about the properties of strongly interacting matter, the role of gluons, and the transition from the hadronic picture of nuclei (i.e. in terms of nucleons and mesons) to quark and gluon (partonic) degrees of freedom [23]. Here we describe some parts of the scientific program in CLAS focused on using the nucleus as a laboratory to test QCD: short-range correlations, three-body forces, and scaling in photoproduction. We also describe the facilities at Jefferson Lab including the CLAS detector.

2 Experimental Facilities

The main scientific instrument at JLab is the continuous electron beam accelerator facility (CEBAF) made of 338 accelerating cavities which produce electrons of energy up to 6 GeV by recirculating the beam up to five times through two superconducting linacs. The maximum current is 200 µA with an energy precision of 10^{-4}, a polarization of $\approx 85\%$, and a duty cycle of 100%. The beam can by simultaneously injected into three end stations: Halls A, B, and C. The CLAS is located in Hall B and has an acceptance covering most of 4π. See Fig. 1.

Its unique toroidal, superconducting magnet is divided into six identical sectors [18]. Each sector consists of drift chambers to measure charged particle trajectories (dark blue, green, and light blue central regions in

G. P. Gilfoyle (✉)
Physics Department, University of Richmond, Richmond, VA 23173, USA
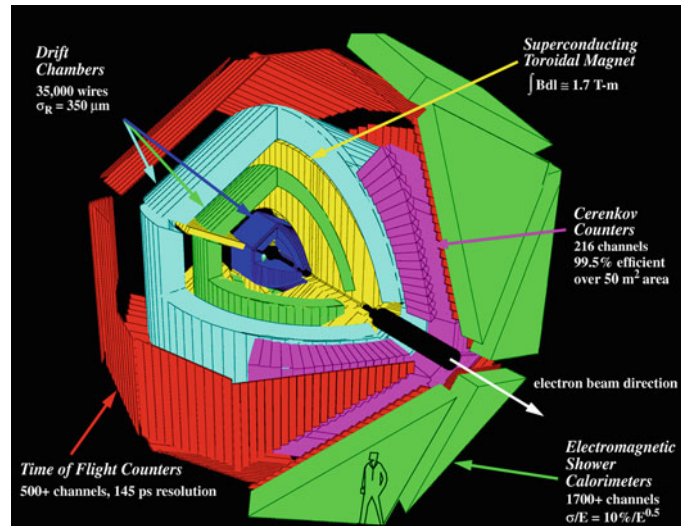E-mail: ggilfoyl@richmond.edu

Fig. 1 Cutaway view of the CLAS detector

Fig. 1), a Cerenkov counter to separate electrons and π^-'s (purple), scintillators to measure time-of-flight (red), and an electromagnetic calorimeter (green, outer layer). Two of the sectors have an additional, large-angle calorimeter. The momentum resolution of CLAS is $\Delta p/p = 0.5\%$ at forward angles and it can operate at a luminosity of 10^{34} cm^{-2}s^{-1}. The angular resolution for charged particles is about 0.05 mr. Charged particles that can be identified are: p, π^+/π^-, K^+/K^-, e^+/e^- over the angular range $8° - 144°$. Neutral particles can be detected over the range $8° - 70°$. Experiments with CLAS require wide kinematic coverage and multiple-particle final states. A photon tagger upstream from CLAS provides photons of known energy over the range $0.2 - 0.95$ of the beam energy up to 6 GeV with a tagger resolution $\Delta E/E \approx 10^{-3}$ [30].

3 Short Range Correlations in Nuclei

Nuclei have long been treated as a collection of individual nucleons bound together by the mean field created by all the other nucleons. This picture accounts for only about 70% of the nuclear charge with much of the discrepancy located at high momentum [16]. To probe these high-momentum components of the nuclear wave function one can search for nucleon pairs and triplets; the high momentum of one nucleon is balanced by the others. By the uncertainty principle these correlated pairs and triplets come from small regions and hence correspond to cold, dense, high-momentum components of the nucleus. They are relevant not only to the study of nuclear structure, but to the physics of neutron stars [14] and the EMC effect [27].

To identify the SRCs is an experimental challenge because they can be obscured by inelastic reactions, final state interactions (FSI), and scattering from low-momentum, uncorrelated nucleons. The first generation of experiments at JLab (and in CLAS) to measure the SRCs relied on inclusive electron scattering with kinematic constraints (i.e., $x_{BJ} > 1$) to reduce these backgrounds [13]. The chances for each nucleon to be a member of an SRC pair was found to be as high as 23%, i.e. each nucleon spent about one-quarter of the time correlated with another nucleon. There was some variation in this probability among different nuclei. Second generation experiments in Hall A at JLab and at Brookhaven National Laboratory (BNL) used exclusive reactions to study isospin effects and found that pn pairs are about 18 times more common that pp pairs [24,33].

Next generation SRC measurements have been performed with CLAS at electron beam energies of 2.2 and 4.7 GeV. The ^{3}He(e, e'pp)n reaction has been measured over a wide kinematic range to study the pp/pn ratio as a function of total pair momentum [7]. SRCs were selected by picking one 'fast' nucleon along the direction of the 3-momentum transfer **q** (i.e. $p_\perp < 0.3$ GeV/c) to minimize FSI and measuring the momenta of the remaining, spectator, pn pair. FSI can form a large background that distorts the SRC signal so it is essential to get it under control [3]. The left-hand panel of Fig. 2 shows distribution of the opening angle between the pn pair with different cuts applied.

Requiring the fast proton to be emitted along the 3-momentum-transfer **q** selects events where that fast proton has not rescattered. This constraint dramatically alters the pn opening-angle distribution; the two nucleons
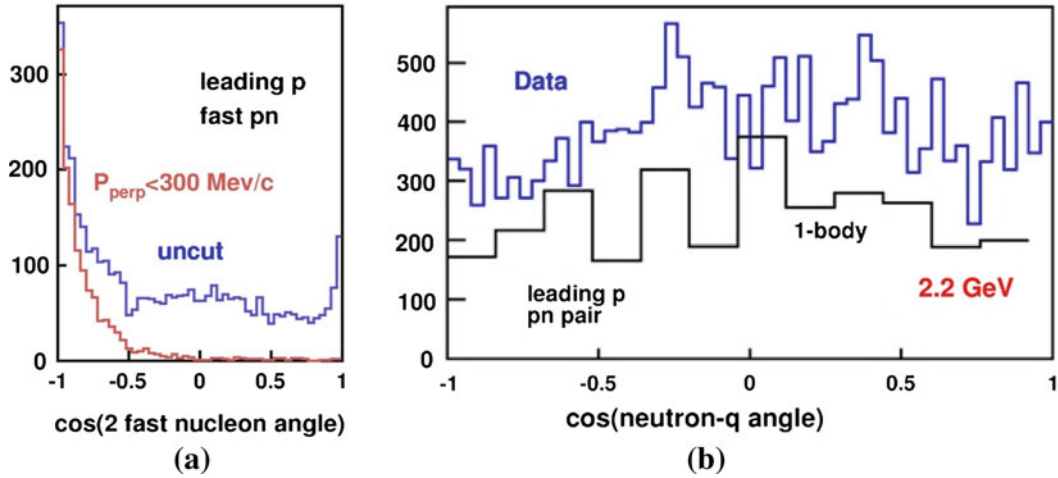
Fig. 2 Angular distribution for *pn* opening angle (*left-hand side*) and neutron angular distribution (*right-hand side*) relative to **q**

now come out back-to-back as expected for a correlated pair (red histogram). The right-hand panel of Fig. 2 shows the neutron angle with respect to **q**. It is isotropic implying the coincidence with the fast proton does not alter the interaction of the *pn* pair. The distribution is also reproduced by a one-body calculation [17]. These results along with the observation that the total pair momentum is small relative to q indicate the *pn* pair's nuclear momentum distribution has been observed (black squares Fig. 3).

Integrating over this distribution in Fig. 3 one obtains a *pp/pn* ratio of about 1:4 instead of 1:18 as seen in Ref [33]. The CLAS results are, in fact, consistent with simple pair counting. To understand this apparent contradiction the dependence of the ratio as a function of the total momentum of the pair was examined (see Fig. 3). The CLAS data are the black squares and the curves (solid and dashed) are calculations from [17]. The *pp/pn* ratio is low (close to 1:18) at small p_{tot} and then increases to the value expected for pair counting in ^{3}He (dotted line). The red line shows *pp/pn* ratio and the range of the Hall A/BNL measurements. The CLAS points overlap this line; consistent with the Hall A/BNL measurements. To understand what is happening the dependence of the *pp/pn* ratio was calculated in Ref [28]. At low total momentum p_{tot} there is a deep minimum in the *pp* cross section so it is smaller than the *pn* cross section, i.e. low *pp/pn* ratio as seen in Fig. 3 and Ref. [33]. As p_{tot} increases the tensor part of the nuclear force fills in this minimum and the *pp/pn* ratio rises; eventually reaching the pair counting value.

Short-range correlations are an important next-step to fully understand atomic nuclei especially in the high-momentum part of the nuclear wave function. SRCs account for up to 23% of the ground state cross section and are dominated by *pn* pairs at $p_{tot} < 0.25$ GeV/c. At high momentum the *pp* cross section rises a level consistent with pair counting. The tensor force is largely responsible for this high-momentum behavior.
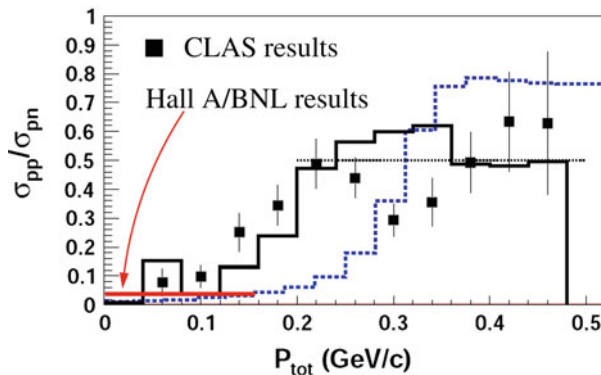

Fig. 3 Ratio of σ_{pp} to σ_{pn} cross section measured with CLAS (*black squares*) versus previous data (*red line*). Curves are discussed in the text. These results have been accepted for publication in Physical Review Letters

4 Few-Body Forces

The NN force in nuclei has a significant two- and three-body component that challenges our understanding of the nuclear ground state and the effect of the nuclear medium. The CLAS program includes a variety of analysis projects studying the breakup of ^{3}He and ^{4}He nuclei using tagged photons with CLAS that are attempting to answer these questions.

The experimental situation for many-body forces in ^{3}He and ^{4}He nuclei is complex. In the ^{4}He(γ, p)t reaction a calculation by Laget including two- and three- body forces describes the data well, but for ^{3}He(γ, d)p Laget overpredicts the three-body contribution by a factor of two [21]. The ^{4}He(γ, p)t results complement the previous study of the three-body breakup ^{3}He(γ, pp)n which illustrated the importance of three-body mechanisms at higher photon energy ($E_\gamma = 0.6 - 0.8$ GeV) [22]. The theoretical calculations follow a diagrammatic approach where the elementary amplitudes are parameterized to include the absorptive effects due to coupling to more and more channels at the energy increases. This feature makes the interpretation model dependent, but provides an essential starting point for further study of the nuclear ground state.

To extend the study the two- and three-body effect in ^{3}He(e, e'pp)n events are selected using a Dalitz plot based on the variables

$$x = \frac{T_{p1} - T_{p2}}{\sqrt{3}\, T_{tot}} \qquad y = \frac{T_n}{T_{tot}} \tag{1}$$

where T_{p1}, T_{p2}, and T_n are the kinetic energies of the two protons and the neutron and T_{tot} is the total.

The left-hand-side of Fig. 4 shows the coordinates for the Dalitz plot and the arrows point to regions where different reaction mechanisms will predominate. For example, when the neutron energy is low ($y \approx 0$) and the remaining energy is evenly split between the two protons ($x \approx 0$) we are in a region dominated by quasi-two-particle forces with the neutron acting as a spectator. In the middle region of the Dalitz plot (the green hexagon in Fig. 4) the energy is shared equally among all three nucleons whose momentum vectors are at $120°$ to one another (the star configuration). Here, three-body mechanisms are expected to be important and the effect of two-body forces is suppressed. Applying cuts to these different regions of phase space enables one to extract the ratio of three-body/two-body strength shown in the right-hand-side of Fig. 4 as a function of incident photon energy.

Comparing an elementary process like meson production on a free nucleon with the same process embedded in a nucleus is a test for understanding the effects of the nuclear medium. Pion production is an essential probe of the long-range part of the NN force, but has not been studied at the photon energies accessible with CLAS. The differential cross section of the reaction ^{3}He(γ, π^+t) has been measured for energies above the Δ resonance with CLAS. This particular reaction is important for comparing with the elementary process on the nucleon because it shares the same quantum numbers as that reaction and hence the same nuclear wave functions (except for Coulomb effects). Figure 5 shows some of the results as a function of Q^2 and for a fixed pion angle of $137°$ in the c.m. frame. The CLAS results are the open circles at high Q^2 and the filled circles
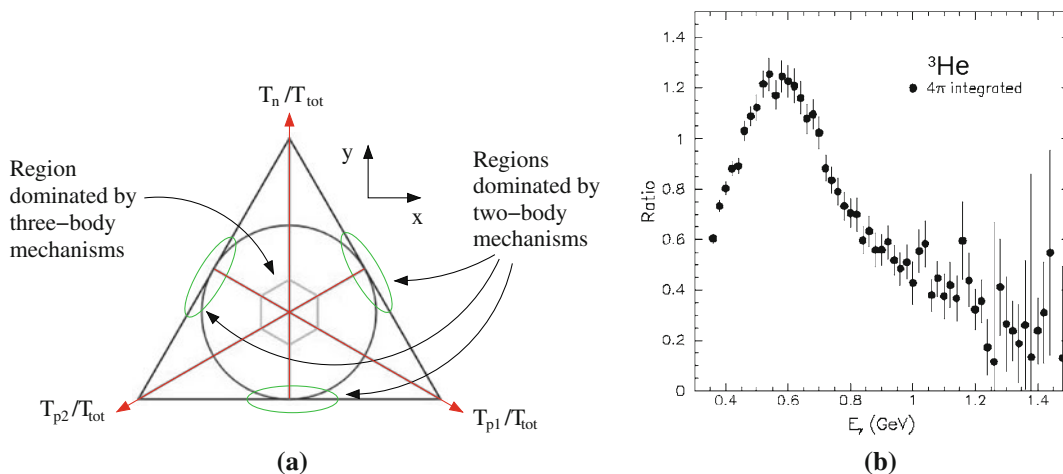

Fig. 4 Dalitz plot (*left-hand-side*) used to select regions of phase-space where two- and three-body forces will predominate and extract the ratio of the production from three-body to two-body forces (*right-hand-side*) as a function of photon energy
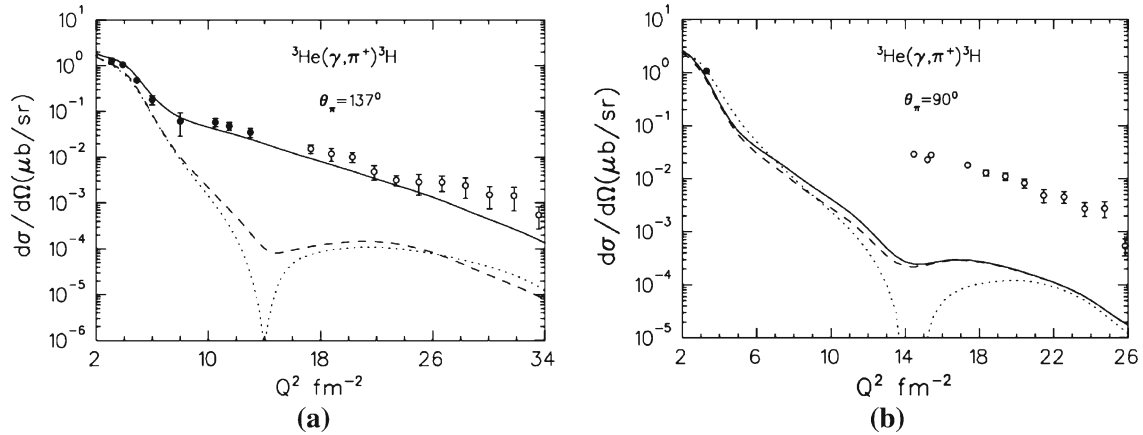
Fig. 5 Comparison of preliminary CLAS results (*open circles*) with previous data ([5,6]) and calculations by Tiator and Kamalov [34] at two different pion c.m. angles. These results have been submitted for publication [20]

are from Refs. [5,6]. While there is no overlap with the previous data in the left-hand panel, the CLAS data agree with the trend of those results. The curves are calculations by Tiator and Kamalov that have recently been extended to higher energies above the previous limit of the Δ region using MAID [34]. The calculations are for the plane-wave impulse approximation PWIA (dotted), distorted-wave impulse approximation DWIA (dashed), and DWIA + 2-body mechanism (solid). The agreement between the data and the calculations in the left-hand panel of Fig. 5 is quite good. However, when other, larger-angle pions are selected one obtains the results shown in the right-hand panel 5. There is a large discrepancy between data and calculations (up to a factor of 10^2 for some Q^2). Other CLAS data at even larger pion angle show similar behavior. This disagreement suggests that important effects have not been included like three-body forces or the presence of preformed Δ resonances [32].

To conclude, there is a significant program using the CLAS detector to study the effects of two- and three-body forces in light nuclei and possible medium modifications to elementary processes. The measurements clearly show the importance of these effects and the recent, preliminary results for the ^{3}He(γ, π^+t) point to the need for additional theoretical work to fully understand these data.

5 Scaling in Photodisintegration of Nuclei

Scaling is one of the iconic signatures for the presence of partons withing the nucleon or nucleus. At high enough momentum, an electron will scatter elastically off one of the constituent partons of a nucleon and its cross section (or some appropriate ratio) will no longer vary with the square of the momentum transfer. This independence of Q^2 is a sign that the parton is a point particle. One of the central goals of JLab is to observe the transition from a hadronic picture of nuclei (nucleons and meson) to one based on partons (quarks and gluons) and to map out that transition. There are important signs that this transition has been observed, but the geography is more complex than anticipated.

Brodsky and Farrar predicted the angular distribution for the process $AB \rightarrow CD$ would follow constituent counting rules (CCR) [11]

$$\frac{d\sigma}{dt}_{AB \rightarrow CD} \approx s^{2-n} f(t/s) \tag{2}$$

where t and s are the total energy and 4-momentum transfer squared (Mandelstam variables) for $s \rightarrow \infty$ and t/s fixed. The number n is the total number of leptons, photons, and quark components. A search for this type of behavior was done using photodisintegration of the deuteron; the $d(\gamma, p)n$ reaction reaches high momentum transfers even at relatively low photon energy [26]. Figure 6 shows some of those results. For the high-angle distributions (see Fig. 6) and $E_\gamma > 1.5$ GeV, the scaled cross section is flat; a sign of scaling. However, CCR are valid for $t \approx s >> m^2$ and are not expected to be valid in the few-GeV region. In addition, several theoretical interpretations exist that describe these data [9,12,15]. For example, the HRM model relies on a quark exchange mechanism and the short distance aspects of the deuteron wave function are not important
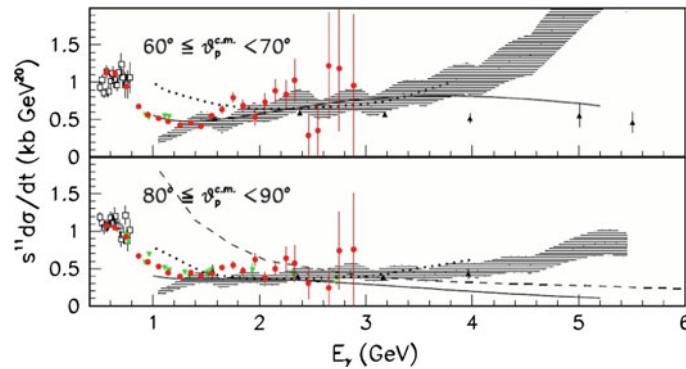
Fig. 6 Photon energy dependence of the scaled cross section for different proton angle bins from CLAS (*red*), Hall C (*blue*) [8,29], and lower energy data from Mainz and SLAC

[15]. The quark-gluon string model (QGSM) uses a topological expansion in QCD and a space-time picture of interactions between hadrons that takes into account the confinement of quarks. Both of these approaches do reasonably well at describing the high-E_γ data.

To distinguish among these different calculations requires additional observations. A CLAS analysis of existing data from 2007 has been approved and is going forward [4]. The idea here is to use spin-dependent effects in deuteron photodisintegration, i.e. the azimuthal, beam-spin asymmetry to challenge theory. This asymmetry is defined as

$$\Sigma = \frac{1}{P_\gamma} \frac{N_\parallel - N_\perp}{N_\parallel + N_\perp} \tag{3}$$

where $N_\parallel$ and $N_\perp$ are the number of events parallel and perpendicular to the linear polarized photon beam respectively. The beam polarization is P_γ. The existing data on Σ are sparse and have large uncertainties [1,2]. A preliminary analysis of 1% of the existing data for the angle bin $80° < \theta_{cm} < 100°$ and energy bin $1.3 < E_\gamma < 1.5$ GeV permitted the extraction of Σ as shown in Fig. 7. These preliminary results are consistent with the previous Yerevan results [1,2]. The anticipated uncertainties are displayed on the red triangles at the bottom of the plot and are small enough to distinguish among the models.

Other pathways exist for exploring the hadronic to quark-gluon transition. In particular, the program described above for the photodisintegration of the deuteron can be extended to ^{3}He [10]. Data have been collected in Hall A that are complemented by some of the CLAS analyses like those in Section 4 [25,31]. These results exhibit scaling behavior at large proton angle $\theta_{cm} > 60°$ and photon energy ($E_\gamma > 2$ GeV) [19]. The proton-proton cross section is 20 times smaller than the proton-neutron one in photon disintegration which can be reproduced by the HRM [15]. This agreement could mean we see scaling in ^{3}He, but alternative explanations like the influence of the tensor force (see Section 3) remain open questions.
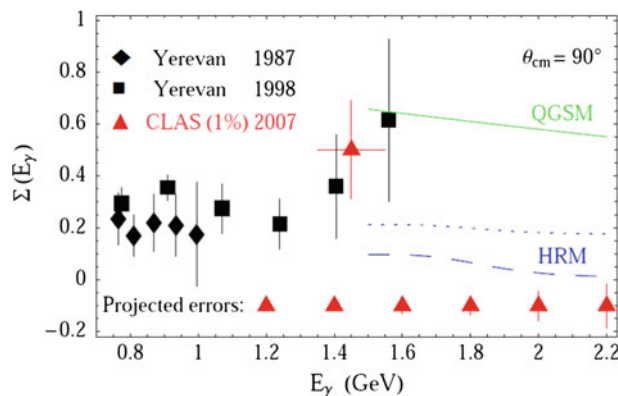

Fig. 7 Comparison of preliminary result for $\Sigma(90°)$ with available experimental data and theoretical predictions
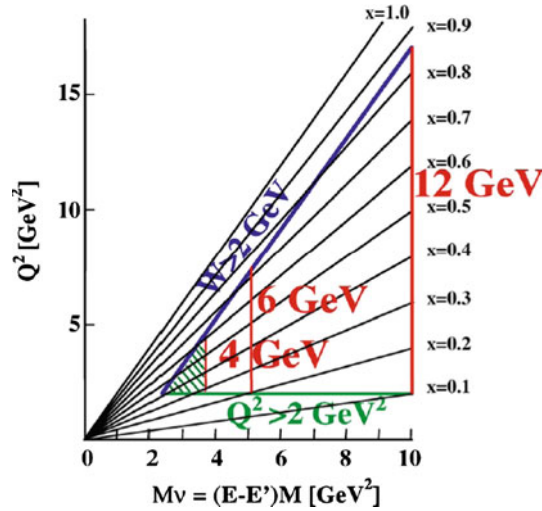
Fig. 8 Kinematic range of the CLAS12 detector after the 12-GeV Upgrade

It now appears that we have reached the transition region where our description of nuclei require quark-gluon degrees of freedom to obtain the full picture. The geography of that transition is more complex than originally expected and there are alternative explanations that will have to be reconciled with new data. Ongoing analysis of deuteron photodisintegration and the breakup of ^{3}He and ^{4}He nuclei will shed new light on these questions. It is also worth pointing out here the synergy among the different halls at JLab. The first signs of scaling behavior seen in CLAS [26] were extended and confirmed in Hall A [25] at higher photon energies. The low E_γ part of the Hall A results were, in turn, confirmed by preliminary CLAS results on ^{3}He(e, e'pp)n.

6 Concluding Remarks

Jefferson Lab has a strong and diverse program that includes a significant component studying few-body physics. The work described here shows that short-range correlations fill in a large hole in our understanding of the nuclear ground state and the influence of the tensor part of the nuclear force is now starting to come into focus. Progress has been made in understanding the impact of two- and three-body forces in light nuclei and the effect of the nuclear medium on pion production. We have likely reached the transition region where the hadronic picture gives way to the quark-gluon one, but its geography is more rugged than expected. It is bears noting the CLAS program also includes studies of color transparency, searches for preformed Δs in nuclei, and three-nucleon SRCs.

The future is bright. Ongoing analysis have been mentioned above and another effort has begun to obtain support for a 'data mining' project to investigate a number of the topics discussed here using existing CLAS data [35]. In addition, JLab is now in the midst of the 12-GeV Upgrade which will double the electron beam energy and build a new detector in Hall B (CLAS12). Figure 8 shows the expansion of the kinematic reach of CLAS12.

The Q^2 coverage and energy transfer range will more than double. A new hall (Hall D) will be added to house a large-acceptance detector built around a solenoidal magnet for photon beam experiments. Specific proposals have already been approved for running in the first five years to study SRC (PR12-06-105) and color transparency (PR12-06-106 and PR12-06-107). There is much more to come with CLAS and in the future with CLAS12.

References

1. Adamian, F., et al.: Deuteron photodisintegration by linearly polarized photons in the energy region 0.3–1.0 GeV. J. Phys. G **17**, 1189 (1991)
2. Adamian, F., et al.: Measurement of the cross-section asymmetry of deuteron photodisintegration process by linearly polarized photons in the energy range $E_\gamma = 0.81.6$ GeV. Eur. Phys. J. A **8**, 423 (2000)

3. Amado, R., Woloshyn, R.: Constraints on the high momentum behavior of inelastic scattering amplitudes. Phys. Lett. B **69**, 400 (1977)
4. Avakian, R., et al.: Determination of the azimuthal asymmetry in deuteron disintegration by linearly polarized photons at $E_\gamma = 1.1 \to 2.3$ GeV. CAA-NP07-01, Jefferson Lab, Newport News (2007)
5. Bachelier, D., et al.: Pion photoproduction on ^{3}He at and above the 3-3 resonance. Phys. Lett. B **44**, 44 (1973)
6. Bachelier, D., et al.: Coherent π^+ photoproduction on ^{3}He in the region of the (1236) resonance. Nucl. Phys. A **251**, 433 (1975)
7. Baghdasaryan, H., et al.: Tensor correlations measured in ^{3}He(e, e'pp)n. (2010) arXiv 1008.3100v1
8. Bochna, C., et al.: Measurements of Deuteron Photodisintegration up to 4.0 GeV. Phys. Rev. Lett. **81**(21), 4576–4579 (1998)
9. Brodsky, S., Hiller, J.: Erratum: reduced nuclear amplitudes in quantum chromodynamics. Phys. Rev. C **30**(1), 412 (1984)
10. Brodsky, S., et al.: Hard photodisintegration of a proton pair in ^{3}He. Phys. Lett. B **578**, 69 (2004)
11. Brodsky, S.J., Farrar, G.R.: Scaling laws at large transverse momentum. Phys. Rev. Lett. **31**(18), 1153–1156 (1973)
12. Diepernik, N.: Photodisintegration of the deuteron in the few GeV region using asymptotic amplitudes. Phys. Lett. B **456**, 9 (1999)
13. Egiyan, K.S., et al.: Measurement of two- and three-nucleon short-range correlation probabilities in nuclei. Phys. Rev. Lett. **96**(8), 082501 (2006)
14. Frankfurt, L., Strikman, M.: Short-range nucleon correlations and neutrino emission by neutron stars. AIP **1056**, 241–247 (2008)
15. Frankfurt, L.L., Miller, G.A., Sargsian, M.M., Strikman, M.I.: QCD rescattering and high energy two-body photodisintegration of the deuteron. Phys. Rev. Lett. **84**(14), 3045–3048 (2000)
16. Gao, J., et al.: Dynamical relativistic effects in quasielastic $1p$-shell proton knockout from ^{16}O. Phys. Rev. Lett. **84**(15), 3265–3269 (2000)
17. Golak, J., Kamada, H., Witała, H., Glöckle, W., Ishikawa, S.: Electron induced pd and ppn breakup of ^{3}He with full inclusion of final-state interactions. Phys. Rev. C **51**(4), 1638–1647 (1995)
18. Mecking, B.A., et al.: The CEBAF large acceptance spectrometer (CLAS). Nucl. Instrum. Method A **503**, 513–553 (2003)
19. Mirazita, M., et al.: Complete angular distribution measurements of two-body deuteron photodisintegration between 0.5 and 3 GeV. Phys. Rev. C **70**(1), 014005 (2004)
20. Nasseripour, R.: Private communication (2010)
21. Nasseripour, R., et al.: Photodisintegration of ^4He into $p + t$. Phys. Rev. C **80**(4), 044603 (2009)
22. Niccolai, S., et al.: Complete measurement of three-body photodisintegration of ^{3}He for photon energies between 0.35 and 1.55 GeV. Phys. Rev. C **70**(6), 064003 (2004)
23. Nuclear Science Advisory Committee. The frontiers of nuclear science. US Department of Energy (2007)
24. Piasetzky, E., et al.: Evidence for strong dominance of proton–neutron correlations in nuclei. Phys. Rev. Lett. **97**, 162504 (2006)
25. Pomerantz, I., et al.: Hard photodisintegration of a proton pair. Phys. Lett. B **684**, 106 (2010)
26. Rossi, P., et al.: Onset of asymptotic scaling in deuteron photodisintegration. Phys. Rev. Lett. **94**(1), 12301 (2005)
27. Sargsian, M., et al.: Hadrons in the nuclear medium. J. Phys. G **29**, R1 (2003)
28. Schiavilla, R., Wiringa, R.B., Pieper, S.C., Carlson, J.: Tensor forces and the ground-state structure of nuclei. Phys. Rev. Lett. **98**(13), 132501 (2007)
29. Schulte, E.C., et al.: Measurement of the high energy two-body deuteron photodisintegration differential cross section. Phys. Rev. Lett. **87**(10), 102302 (2001)
30. Sober, D., et al.: The bremsstrahlung tagged photon beam in Hall B at JLab. Nucl. Instrum. Method A **440**, 263 (2000)
31. Strauch, S.: Private communication (2010)
32. Strueve, W., et al.: ^{3}He and 3H electromagnetic form factors. Nucl. Phys. A **465**, 651 (1987)
33. Subedi, R., et al.: Probing cold dense nuclear matter. Science **320**, 1476–1478 (2008)
34. Tiator, L., Kamalov, S.: Private communication (2010)
35. Weinstein, L., Kuhn, S., et al.: Short distance structure of nuclei—mining the wealth of existing Jefferson lab data. Tech. rep., US DOE, Office of Nuclear Physics (2009)